Journal of Pharmaceutical Sciences 105 (2016) 1858–1866

Contents lists available at ScienceDirect

Journal of Pharmaceutical Sciences

journal homepage: www.jpharmsci.org

Pharmaceutics, Drug Delivery and Pharmaceutical Technology

Survival of the Fittest: Time-To-Event Modeling of Crystallization of Amorphous Poorly Soluble Drugs

Katarzyna Nurzyńska [1,*], Rupert P. Austin [1], Peter M. Fischer [2], Jonathan Booth [3], Frank Gommer [4]

[1] BAST Inc. Ltd., Holywell Park, Ashby Road, Loughborough, UK LE11 3AQ
[2] School of Pharmacy and Centre for Biomolecular Sciences, The University of Nottingham, Nottingham, UK NG7 2RD
[3] Pharmaceutical Development, AstraZeneca, Macclesfield, UK SK10 2NA
[4] Composites Research Group, Faculty of Engineering, The University of Nottingham, Nottingham, UK NG7 2RD

ARTICLE INFO

Article history:
Received 24 October 2015
Revised 6 March 2016
Accepted 11 March 2016

Keywords:
amorphous
crystallization
stability
poorly soluble drug
prediction

ABSTRACT

The objective of this study was to gain a quantitative understanding of the link between physicochemical properties and long-term and time-censored amorphous stability of poorly water-soluble drugs using parametric time-to-event modeling. Previously published data on amorphous stability and physicochemical properties of 25 structurally diverse neutral, poorly soluble compounds were used. To describe the general shape of the survival curve (probability of event at time > t), Constant, Gompertz, and Weibull hazard functions and their linear combinations were tested. For a selected Weibull hazard base model, the effect of each physicochemical covariate was investigated, with combined influence of enthalpy of fusion (H_f) and molecular weight (M_r) showing the highest statistical significance. The covariate model was used to simulate survival curves and calculate the median survival time for different values of H_f and M_r. It was found that a decrease in H_f or an increase in M_r contribute to longer survival times. The derived model equation was validated against external data sets consisting of 11 compounds. It showed better predictive ability than a previously published multiple linear regression model incorporating H_f and M_r. The proposed Weibull covariate model may assist in faster and more cost-effective decision making in the pre-formulation phase of drug development, where compound properties and appropriate drug formulation strategies are investigated.

Introduction

Small-molecule drug candidates with good pharmacological properties frequently suffer from low aqueous solubility. For oral drug products, this can lead to insufficient and erratic bioavailability of the active pharmaceutical ingredient (API), and for that reason, lipophilic APIs with limiting aqueous solubility are often formulated in the amorphous state, typically as solid dispersions in polymer matrices.[1] This approach is favorable because the amorphous solid state of a molecule is at a higher energy level compared with its crystalline state, giving rise to higher dissolution rates and solution concentrations of poorly soluble APIs from amorphous versus crystalline formulations.[2] However, on account of the comparatively disordered and mobile nature of amorphous solids, APIs can crystallize from amorphous formulations on storage or on contact with gastrointestinal fluids after administration. Such instability is a significant hurdle in the development of new medicines, and it would be highly desirable to be able to predict the inherent amorphous stability of poorly soluble APIs and the stability of such molecules in amorphous solid dispersions.

One physical stability classification methodology assesses the glass-forming ability of APIs after rapid solvent evaporation from a solution or cooling from a melt,[3,4] whereas in a different method the phase transition from the amorphous to a crystalline state is observed directly as a function of time.[5,6] In the former method, the assumption is that some compounds have an inherent ability to form amorphous solids from liquids, whereas others more readily assume a crystalline state on transition from the liquid to the solid state. It has been observed that the crystallization classification of model APIs is similar, independent, however, of methodology. From the limited data published to date, it would appear that the

Conflicts of interest: The authors declare no competing financial interest.
This article contains supplementary material available from the authors by request or via the Internet at http://dx.doi.org/10.1016/j.xphs.2016.03.014.

* *Correspondence to:* (Telephone: 01509222908).
E-mail address: knurzynska@bastinc.eu (K. Nurzyńska).

http://dx.doi.org/10.1016/j.xphs.2016.03.014

crystallization behavior of APIs depends predominantly on the properties of the API and other formulation components, rather than the amorphization methodology itself.[4,7] However, environmental conditions, for example, humidity and temperature, can also affect amorphous drug stability[8] and can, therefore, lead to different results reported by different laboratories. Although the intrinsic factors affecting ease of compound crystallization from the amorphous state, such as molecular mobility and thermodynamic properties of the amorphous state,[9] remain poorly understood, efforts have been underway to correlate observed glass-forming ability or physical stability of amorphous APIs with physicochemical and other properties of the APIs. Some progress has been made in the prediction of the physical stability of amorphous APIs.[6,10-13]

The framework developed on pure APIs in this work can be used as a preliminary risk assessment for the development of their solid dispersion formulations. It is expected that the amorphous stability of solid dispersions will be improved in comparison with pure drugs due to the dilution effect and the presence of specific interactions between a drug and a polymer. Amorphous compounds that are shown to have good amorphous stability should also be stable in their solid dispersions. Conversely, compounds that have poor stability may still be formulated as viable solid dispersions, but the products are likely to have higher risk of crystallization.

In a previous study,[6] the amorphous stability of 25 diverse neutral poorly soluble drug compounds were investigated. Principal component analysis and clustering methods were used to select 25 compounds with diverse physicochemical properties and chemical structures from the database of 533 marketed poorly soluble drugs. The selected sample set was shown to be representative for the calculated and predicted variables as side-by-side histograms for both distributions showed the same mean location and variance.[6] Several multiple linear regression (MLR) models were proposed to predict long-term amorphous drug stability using only easily accessible physicochemical drug properties as covariates. Due to practical limitations, continuous crystallization records during the approximately 6-month period of the experiment were not obtained. Instead, amorphous drug stability was measured at defined time points, with some compounds remaining stable at the end of the experiment. Time-to-event (TTE) modeling, also known as survival analysis,[14,15] is particularly suited to this type of data and was applied in the present study to the previously published data on 25 diverse compounds. Here we present the new application of TTE modeling to more accurately determine the influence of physicochemical parameters on the long-term amorphous stability of poorly soluble compounds.

A central concept in TTE modeling is the survival function $S(t)$, which describes the probability that an event will occur at a time greater than t. The survival function is related to the hazard function $h(t)$, which can be understood as the instantaneous failure rate (onset of amorphous to crystalline transition in this study) given that the compound has survived to that point in time. The survival and hazard functions are related through Equation 1.

$$S(t) = \exp\left(-\int_0^t h(t)\,\mathrm{d}t \right) \quad (1)$$

In parametric TTE modeling, a base model is first derived using a process in which various hazard functions $h(t)$ are proposed, and estimates of the parameters of the hazard functions are determined using maximum likelihood estimation. This involves integration of the hazard function from zero to the time of each crystallization event, giving the contribution of each event to the total likelihood, where the parameter estimates are derived by maximizing the sum of all likelihood contributions with respect to the parameter values. This estimation process is applied to each of the candidate hazard functions, and the best function is selected based on model selection criteria and graphical comparison of observed and predicted data. Once a hazard function has been selected, a covariate analysis is performed where the physicochemical properties of the compounds are allowed to influence the parameters within the hazard function. Model selection criteria are then used to select a final covariate model where the included covariates produce a statistically significant improvement compared with the base model. The model can then be used to simulate the expected behavior of new compounds with different values of the included covariates.

Methods

Software

The TTE models were developed using NONMEM software,[16] version 7.3 (Icon Development Solutions, Ellicott City, MD). All other analyses and visualization of data were implemented using R software[17] and use of the "survival" library, version 2.38,[18] and the "deSolve" library, version 1.11.[19]

Database Preparation

Previously published data of physicochemical properties and amorphous stability of 25 compounds[6] were used to derive a TTE model. For 17 of the compounds, the precise time of detectable transition from amorphous to crystalline structure is unknown. It was only recorded that the transition took place between 2 observation times. Such data are called interval-censored and were flagged on both sides of the interval within the database used for modeling (Supplementary Material A). For the remaining 8 compounds, observations were flagged as right-censored because crystallization was not observed during the 168 days of experiment. This vector of flag values was used as a dependent variable. The elapsed time of the interval and right-censored observations were included as main independent variable. The following measured, calculated, and predicted physicochemical properties of the 25 compounds[6] were also tested during development of the covariate model: enthalpy of fusion (H_f), glass transition temperature (T_g), melting temperature (T_m), configurational entropy (S_c), enthalpy (H_c) and free energy (G_c), relaxation time (τ), molecular weight (M_r), hydrogen bond donors and acceptors, rotatable bonds (rotB), number of rings, aromatic rings, aliphatic rings, heavy atom count, ratio of carbon to heteroatoms, polar surface area, lipophilicity (clogP), and water solubility ($\log S_w$) predicted both with CLab[6,20] and ALOGPS[21] (www.vcclab.org). These descriptors have been shown in the literature to have an impact on the glass-forming ability and amorphous stability,[3,11] drug bioavailability,[22] and the stability of compounds formulated as solid dispersions.[23]

Model Building and Selection Criteria

For selection of an appropriate base model, 8 different hazard functions were evaluated (Table 1).[24] The hazard functions are defined with parameters λ and β which determine the shape of the hazard function (Supplementary Material B). Because hazard functions must always be positive, the lambda parameters (λ_c, λ_1, and λ_2) were constrained to positive values during parameter estimation, whereas positive or negative estimates of the beta parameters (β_c and β_1) were permitted. The parameter values in the TTE models were estimated using the first-order conditional estimation method,

Table 1
Hazard Functions Tested During Selection of the Base Model

Hazard Function	Definition
Constant	$h(t) = \lambda_c$
Gompertz	$h(t) = \lambda_1 \cdot \exp(\beta_1 \cdot t)$
Weibull	$h(t) = \lambda_1 \cdot \exp(\beta_1 \cdot \ln(t))$
Constant + Gompertz	$h(t) = \lambda_c + \lambda_1 \cdot \exp(\beta_1 \cdot t)$
Constant + Weibull	$h(t) = \lambda_c + \lambda_1 \cdot \exp(\beta_1 \cdot \ln(t))$
Gompertz + Gompertz	$h(t) = \lambda_1 \cdot \exp(\beta_1 \cdot t) + \lambda_2 \cdot \exp(\beta_2 \cdot t)$
Weibull + Weibull	$h(t) = \lambda_1 \cdot \exp(\beta_1 \cdot \ln(t)) + \lambda_2 \cdot \exp(\beta_2 \cdot \ln(t))$
Gompertz + Weibull	$h(t) = \lambda_1 \cdot \exp(\beta_1 \cdot t) + \lambda_2 \cdot \exp(\beta_2 \cdot \ln(t))$

which uses maximum likelihood estimate to minimize the objective function value (OFV) and, thus, obtain the best model fit to the data.[25] The direction in which the OFV decreases to find the global minimum was determined in an iterative process using the gradient method.[26] To ensure convergence to the global minima, models were run repetitively, each time starting from different initial parameter estimates. The global minimum was considered to be reached when all repetitive runs resulted in the same final parameter estimates and OFVs. Estimates of parameter uncertainty (standard error) were generated using the NONMEM covariance procedure.[16]

Models were first required to pass the following acceptance criteria[27]:

1. At the last iteration, the values of the gradients have to be between 10^{-6} and 10 to indicate that the OFV successfully converged to its minimum.
2. The covariance step, where uncertainty in parameter estimates is determined, has to complete successfully.
3. The number of significant digits of parameter estimates has to be $\geq$3.
4. The correlation between estimated parameters, cp, has to be $-0.95 \leq \text{cp} \leq 0.95$. This criterion will reject models that are overparametrized.
5. The ratio of maximum to minimum eigenvalues of the correlation matrix of parameter estimates (condition number) has to be $\leq$1000. This criterion will reject models that are overparametrized.
6. The standard error of each parameter estimate is required to be <50% of the estimated parameter value. This ensures that the 95% confidence interval for the parameter estimate excludes zero.

For those models that passed the acceptance criteria, the base model (Table 1) was then selected using Akaike information criterion (AIC). This criterion is used to compare nonnested models, where fixing one parameter in the first model to its null value is not leading to the second model. According to this criterion (Eq. 2), a model (A) is statistically superior to a model (B) if AIC <0.

$$\text{AIC} = \text{OFV}_{\text{model A}} - \text{OFV}_{\text{model B}} + 2(n_{\text{model A}} - n_{\text{model B}}) \quad (2)$$

where n is the number of model parameters.

The influence of covariates on the parameters of the selected base model was then tested using the forward inclusion method. Covariate effects were assessed one by one followed by evaluation of the combined effect of significant covariates. The effect of each covariate, COV, was modeled relative to the median value of that covariate, $\text{COV}_{\text{median}}$, in the sample set[28] according to Equation 3.

$$\text{COV}_m = \text{COV} - \text{COV}_{\text{median}} \quad (3)$$

Covariate models of 2 different types were tested. When testing the influence of a covariate on a λ parameter, λ as given by the equations in Table 1 was replaced by λ_{cov} as defined by Equation 4

$$\lambda_{\text{cov}} = \lambda \cdot \exp(\theta \cdot \text{COV}_m) \quad (4)$$

where θ is a new parameter, estimated by the modeling software, which quantitatively describes the influence of the covariate on the hazard function. The functional form of Equation 4 enables the possibility that an increase in the covariate can increase or decrease the magnitude of the hazard function (positive or negative estimate of θ) while satisfying the constraint that the hazard function should always be positive. When testing the influence of a covariate on a β parameter, a different functional form of the covariate model was used as defined by Equation 5.

$$\beta_{\text{cov}} = \beta \cdot (1 + \theta \cdot \text{COV}_m) \quad (5)$$

This different functional form allows the possibility of changes in the covariate influencing the magnitude and sign of the original β parameter because both positive and negative values of β_{cov} are permitted (they both lead to a positive hazard function). The forms of Equations 4 and 5 also ensure that if the covariate parameter θ is zero, then the hazard function reduces to that of the base model.

The significance of the covariate models was assessed using the likelihood ratio test (LRT).[14] The covariate was considered to have a significant effect if the decrease in the OFV of the covariate model from that of the base model was >6.63 (p value < 0.01). This stringent p value was used due to the inflated type I error that occurs during multiple testing (testing of many possible covariate relationships). For the final covariate model, the estimates of parameter uncertainty produced by the NONMEM covariance procedure were supplemented by a more thorough bootstrap procedure implemented using PsN software.[29] This involved taking the structure of the final covariate model and repeatedly fitting it to 1000 data sets, each produced by sampling with replacement from the original data set of 25 compounds. This provided 1000 estimates of each model parameter. Then 95% nonparametric confidence intervals were generated from the 2.5 and 97.5 percentiles of the 1000 parameter estimates.

Model Qualification

The final covariate model was qualified using a visual predictive check (VPC), which involves assessment of the concordance between the observed crystallization events and repeated simulations of crystallization events from the selected model.[30-32] To generate the VPC, the selected covariate model was used to simulate 1000 sets of event times for the 25 compounds. Then, using the survival library in R, Kaplan–Meier survival curves with 95% confidence intervals were plotted for the observed events and for the 2.5, 50, and 97.5 percentiles. A good model should show extensive overlap of the confidence intervals derived from the observed and simulated event data with little evidence of bias. The simulated event times were generated through numerical integration (using R library deSolve) of $h(t)$ to give $S(t)$. This was followed by repeated sampling of random numbers from a uniform distribution in the interval 0 to 1 (because $S(t)$ is uniformly distributed on the interval 0 to 1)[24] and finding corresponding times at which the survival function became less than or equal to the sampled random number. Adjustment of the simulated event times according to the scheduled experimental measurement times (1 hour, 3 hours, 1 day, 7 days, 1 month, 2 months, 4 months, and 6 months)[6] was necessary to allow correct comparison with the interval-censored nature of the observed data. For example, if a particular simulated event time was 4.63 days, it would be adjusted to 7 days because that is the first point in time where the crystallization event could have been observed according to the experimental schedule.

Results and Discussion

Selection of the Base Model

The 8 hazard functions tested for selection as base model were Constant, Gompertz, and Weibull functions and their linear combinations (Table 1). Parameter estimates, OFV, and selection criteria status for the 8 candidate base models are given in Table 2. The last 4 models were immediately rejected due to failure of acceptance criteria. Failure was either due to an unacceptably wide standard error in one or more parameter estimates or to unsuccessful completion of the NONMEM covariance procedure that generates the standard errors. The latter occurred due to numerical instability with the Constant + Weibull model where the parameter λ_c optimized to a vanishingly small value. Figure 1 shows the 4 models that passed the acceptance criteria, where the estimated survival curves derived from the models are shown superimposed on the Kaplan–Meier plot of the observed crystallization events. The Weibull and Constant + Gompertz models clearly match the observed Kaplan–Meier curve better than the Constant and Gompertz models. The 2 former models have OFVs that are lower than the latter 2; therefore, a selection between the Weibull and Constant + Gompertz model was the only decision required.

Selection of the base model from the 2 remaining models was initially performed using a consideration of AIC alone. The Constant + Gompertz model has an OFV that is 2.8 units lower than the Weibull model (Table 2) but has 1 additional parameter (Table 1). This leads to an AIC of −0.8 in favor of the Constant + Gompertz model. It should be noted from Table 2 that the standard errors of all 3 parameter estimates in the Constant + Gompertz model are close to 50% of the parameter estimates, whereas the precision of parameter estimates in the Weibull model is considerably better. During early attempts to build covariate models using the initially selected Constant + Gompertz base model, it was soon found that the additional complexity arising from incorporation of covariate models caused all parameters to have standard errors that were >50% of the associated parameter estimate. Due to its additional complexity, the Constant + Gompertz model appears to be less stable than the Weibull model and is likely to be overparameterized when covariates are added. Hence, the selection of the most appropriate base model was reassessed, and the Weibull model was chosen on the basis that it has an OFV only 2.8 units higher than the Constant + Gompertz model. It leads to a similar visual concordance with the observed Kaplan–Meier curve (Fig. 1) but with the advantage of one fewer parameter and more precise parameter estimates.

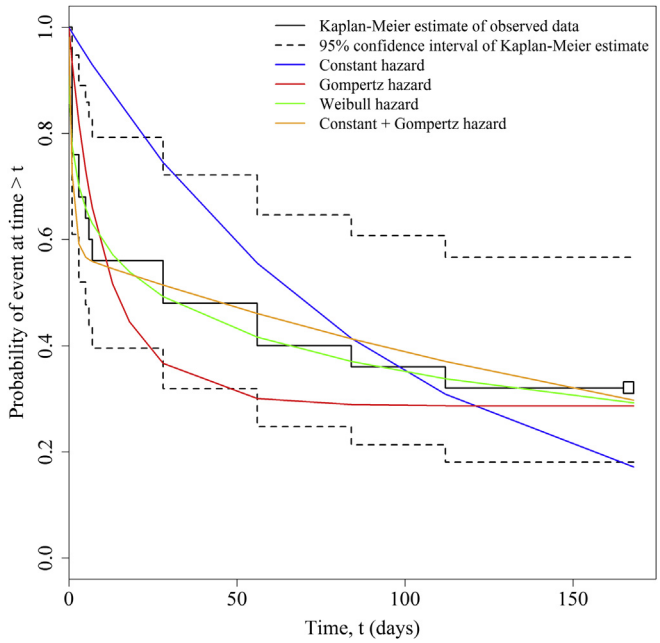

Figure 1. Visual assessment of candidate base models. Kaplan–Meier curve of observed data is shown as continuous black line with 95% confidence intervals shown as black dashed lines. Kaplan–Meier curves of estimated survival functions derived from 4 candidate base models are shown as colored lines.

Selection of the Covariate Model

The individual and combined effects of calculated, predicted, and measured compound properties[6] on the parameters λ_1 and β_1 in the Weibull hazard function were investigated. The LRT was used to decide if incorporation of a particular covariate led to a significant improvement in the model, with the requirement of a decrease in the OFV of the covariate model with respect to the base model of >6.63. Based on this criterion, none of the covariates were found to have a significant effect on β_1 and 4 covariates were found to have a significant effect on λ_1 when tested independently: H_f (ΔOFV = −13.46), M_r (ΔOFV = −10.33), heavy atom count (ΔOFV = −9.79), and number of rings (ΔOFV = −7.84). Furthermore, a model involving the influence of both H_f and M_r on λ_1 gave a further significant decrease in OFV (ΔOFV = −23.91). Additional inclusion of a multiplicative interaction term between H_f and M_r to the latter model did not further improve this model significantly given the use of an additional estimated parameter (ΔOFV = −26.14). Attempts to include either heavy atom count or number of rings as an additional covariate in this model did not lead to a further significant reduction in OFV according to the LRT. This is likely due to heavy atom count and number of rings being significantly correlated with M_r; hence, they are unable to contribute significantly to further explanation of variability in the data. The correlation matrix for all variables used in model selection is shown in Supplementary Material C. The final selected covariate

Table 2
Parameter Estimates and OFV From Base Models

Hazard Function	OFV	10^3 λ_c (d^{-1})	10^3 λ_1 (d^{-1})	10^3 β_1 (d^{-1})	10^3 λ_2 (d^{-1})	10^3 β_2 (d^{-1})	Acceptance Criteria Met
Constant	410142.8	10.5 (2.55)[a]	–	–	–	–	Yes
Gompertz	410107.9	–	72.3 (24.8)[a]	−57.8 (16.5)[a]	–	–	Yes
Weibull	410096.5	–	78.2 (19.4)[a]	−692 (68.5)[a]	–	–	Yes
Constant + Gompertz	410093.7	3.91 (1.60)[a]	475 (227)[a]	−854 (361)[a]	–	–	Yes
Constant + Weibull[b]	410096.5	$<5\times10^{-6}$	78.2	−692	–	–	No
Gompertz + Gompertz	410089.9	–	472 (235)[a]	−926 (415)[a]	13.2 (8.69)[a]	−20.7 (12.3)[a]	No
Weibull + Weibull	410096.5	–	34.8 (3200)[a]	−692 (132)[a]	43.4 (3200)[a]	−692 (114)[a]	No
Gompertz + Weibull	410091.4	–	342 (245)[a]	−847 (457)[a]	36.3 (25.1)[a]	−578 (180)[a]	No

[a] Standard errors of parameter estimates, derived using NONMEM covariance method.
[b] Covariance procedure did not complete successfully.

model, therefore, included the influence of H_f and M_r on λ_1. The hazard function for this model is given in Equation 6 (where 72.92 is the median H_f and 406.56 is the median M_r), the parameter estimates are given in Table 3, and the NONMEM control file is shown in Supplementary Material D.

$$h(t) = \lambda_1 \cdot \exp(\beta_1 \cdot \ln(t)) \cdot \exp\Big(\theta_1\left(H_f - 72.92\right) + \theta_2(M_r - 406.56)\Big) \quad (6)$$

The estimate of parameter θ_1 is positive which indicates that an increase in H_f leads to an increase in $h(t)$ and, hence, a decrease in stability of amorphous compounds. This directional influence is entirely consistent with a larger enthalpy of fusion leading to a greater thermodynamic driving force toward crystallization. Contrarily, θ_2 has a negative estimate such that an increase in M_r leads to an increase in amorphous drug stability. The positive effects of high M_r and low H_f on amorphous stability determined here are consistent with the earlier MLR analysis of the same data set[6] and also with other literature reports.[3,9,10] The MLR study found that both M_r and H_f were individually correlated with amorphous stability ($R = 0.59$ and $R = -0.73$, respectively) and the model equation involving both covariates is given by Equation 7.

$$\log(\text{Stability}) = 0.00309M_r - 0.0265H_f + 1.92. \quad (7)$$

It was previously reported that molecules with high M_r often have a complex structure that impedes orientation in a crystal lattice, which leads to higher stability in a disordered, amorphous state.[3] Molecules with high H_f require more energy to disrupt the crystalline lattice during melting. As melting precedes the formation of the amorphous material, the energy supplied during melting increases the internal energy of the system and, thus, lowers its physical stability.[6]

The 95% confidence intervals around the parameter estimates in Table 3 were derived from a nonparametric bootstrap procedure which involved fitting of the model to 1000 different data sets of 25 compounds, each sampled (with replacement) from the original data set.[29] The distributions of parameter estimates for the 4 model parameters, derived from the bootstrap procedure, are shown in Figure 2, and the 95% confidence intervals in Table 3 were derived from the 2.5 and 97.5 percentiles of each distribution. The 95% confidence intervals around the estimates of λ_1, β_1, and θ_1 all exclude the null value of zero, but the confidence interval around θ_2 does include zero by a small margin. However, the inclusion of θ_2 in the model does satisfy the requirement of the LRT because the OFV reduces by 10.45 on addition of the influence of M_r to a simpler model that only includes the influence of H_f. It is likely that adding more compounds to the sample set for a future analysis would lead to a more precise estimate of θ_2.

It is important to recognize that the generation of events using a TTE model is a stochastic process and repeated simulations of event times from the model will be different and will encompass a range of values.[24] A suitable method for qualification of such a model is the VPC, which involves repeated simulations of the model followed by a visualization (using Kaplan–Meier curves) of the observed events and the range of simulated events.[30] This diagnostic plot helps to ensure that repeated simulations of event times from the model are consistent with the observed event times, without evidence of significant bias. A VPC of the selected Weibull covariate model was generated using 1000 repeated simulations of event times for the set of 25 compounds. The results are shown in Figure 3, which indicates a very good concordance between the Kaplan–Meier curve (and associated 95% confidence interval) of the observed crystallization events and the median of the 1000 Kaplan–Meier curves (and associated 95% confidence interval) derived from simulated data. There is substantial overlap between the 2 sets of confidence intervals, and there is no indication of any significant bias, which could be observed in different relative positions of observed and simulated Kaplan–Meier curves over long periods of time. This confirms that the selected Weibull covariate model gives a good description of the experimental data.

Table 3
Parameter Estimates of the Selected Weibull Covariate Model

Parameter	Estimate	95% Confidence Interval From Bootstrap
λ_1 (1/d)	0.0630	0.0246: 0.110
β_1 (1/d)	−0.458	−0.574: −0.181
θ_1 (g/J)	0.0560	0.0381: 0.0999
θ_2 (mol/g)	−0.00771	−0.0148: 0.00341

Sensitivity Analysis

A sensitivity analysis was performed to investigate and visualize the effect of the selected covariates on the expected median event time for crystallization. The Weibull covariate model hazard function (Eq. 6) was analytically integrated to generate the associated survival function (Eq. 1).[24] The resulting survival function is given by Equation 8

$$S(t) = \exp\left(-\frac{K \cdot t^{\beta_1+1}}{\beta_1 + 1}\right) \quad (8)$$

where K is given by Equation 9

$$K = \lambda_1 \cdot \exp\Big(\theta_1\left(H_f - 72.92\right) + \theta_2(M_r - 406.56)\Big). \quad (9)$$

The expression for $S(t)$ given by Equation 8 can now be plotted for different values of H_f and M_r to explore the sensitivity of $S(t)$ to ±20% changes in H_f and M_r around values of 100 J/g and 500 g/mol, respectively. Given that the model contains significant uncertainty in the estimates of the 4 parameters in Equation 6, it was decided that parameter uncertainty should be incorporated into the sensitivity analysis. Hence, for each fixed pair of M_r and H_f values, $S(t)$ was calculated 1000 times using the 1000 sets of parameter estimates derived from the bootstrap procedure. At each time point, the median of the 1000 $S(t)$ values was calculated along with 80% confidence intervals leading to the plots shown in Figure 4. These plots indicate that 20% changes in both H_f and M_r lead to highly significant changes in the survival curves for amorphous stability. The sensitivity to changes in H_f is greater than changes in M_r such that the example ±20% changes in H_f lead to 7.9-fold changes in median crystallization time, whereas ±20% changes in M_r lead to 4.1-fold changes in median crystallization time. Note that Figure 4b contains significantly wider confidence bands than Figure 4a, and this is related to the greater uncertainty in estimation of θ_2 compared with θ_1 (Table 3).

If parameter uncertainty is neglected, the sensitivity analysis can be reduced to a simpler format by taking the expression for $S(t)$ in Equation 8, setting it equal to 0.5, and then solving the equation for t, which is equivalent to finding the median crystallization time rather than the entire survival curve including parameter uncertainty for a particular combination of both H_f and M_r. This leads to Equation 10

$$t = \exp\left(\left(\frac{1}{\beta_1 + 1}\right) \cdot \ln\left(\frac{-(\beta_1 + 1) \cdot \ln(0.5)}{K}\right)\right) \quad (10)$$

The median crystallization time for various combinations of H_f and M_r was calculated using Equation 10 and is shown in Table 4. The explored ranges of H_f and M_r led to a 17,000-fold range in

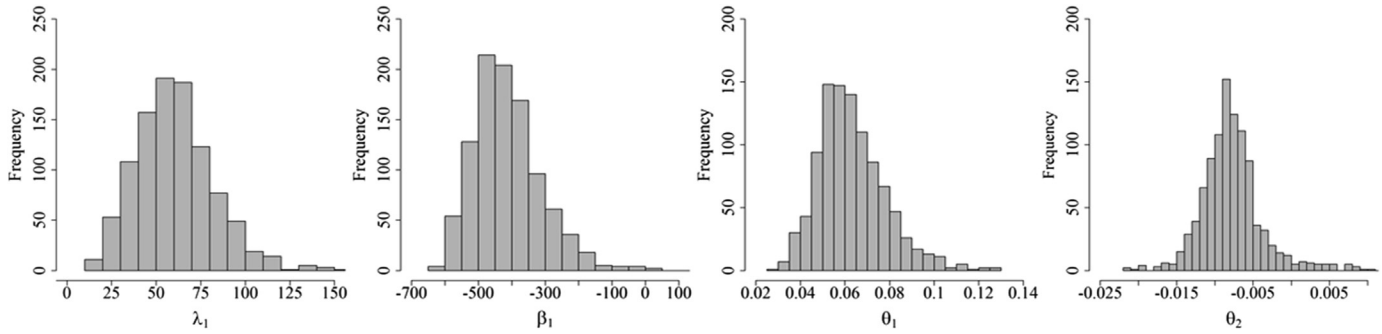

Figure 2. Distributions of parameter estimates derived from bootstrap analysis of Weibull covariate model.

amorphous stability. These results further demonstrate the large influence that H_f and M_r are expected to have on the amorphous stability of compounds with different properties.

It should be remembered that the generation of predictions using a TTE model is a stochastic process (even when parameter estimates are very precise), and once a model has been derived, the process of predicting event times involves the drawing of samples from a probability distribution. Hence, the crystallization times listed in Table 4 represent the median expected crystallization times that might be observed for large populations of compounds representing each of the combinations of H_f and M_r. There will be considerable variation in the predicted crystallization times of particular compounds around each of the median values. This is consistent with reports in the literature that compounds with similar physicochemical properties and chemical structure can demonstrate very different amorphous stability.[8] This is also true for the data set studied here, for example, celecoxib (H_f = 72.2 J/g, M_r = 358.8 g/mol, stable for 6 days) and etoricoxib (H_f = 84.1 J/g, M_r = 381.4 g/mol, stable for 84 days).

Validation on External Data Sets

A test set of 11 compounds, obtained from the literature[3] and from AstraZeneca,[6] was used to validate the derived Weibull covariate model. The observed crystallization times of the 11 test set compounds are given in Table 5. Because only the time of first detection of crystallization was known for these compounds, without knowledge of the time of the previous observation where crystallization was not detected, the crystallization times are less informative than the interval-censored data used for building the model. The Weibull covariate model was used to predict 1000 sets of crystallization times for the 11 compounds, and the observed and simulated events are displayed in Figure 5 using the same display format as that used for the VPC in Figure 3. This shows considerable overlap of the 95% confidence intervals derived from the observed and predicted data and exhibits a very similar shape of the observed and median predicted Kaplan–Meier curves. Therefore, the range of crystallization event times predicted by the Weibull covariate model are consistent with the observed event times, which indicates that the model has the ability to generate useful quantitative predictions

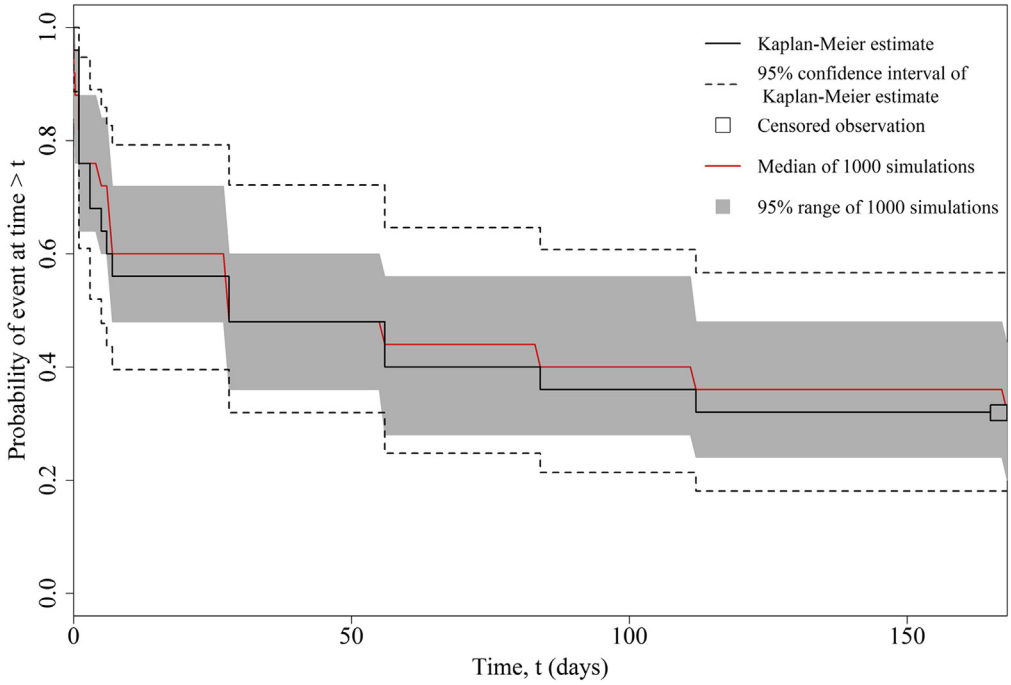

Figure 3. VPC of the selected covariate model showing Kaplan–Meier curves of observed events (black line) and median of simulated events (red line). The dashed lines indicate the 95% confidence intervals of observed events and the gray shading show the 95% confidence interval of the simulated events.

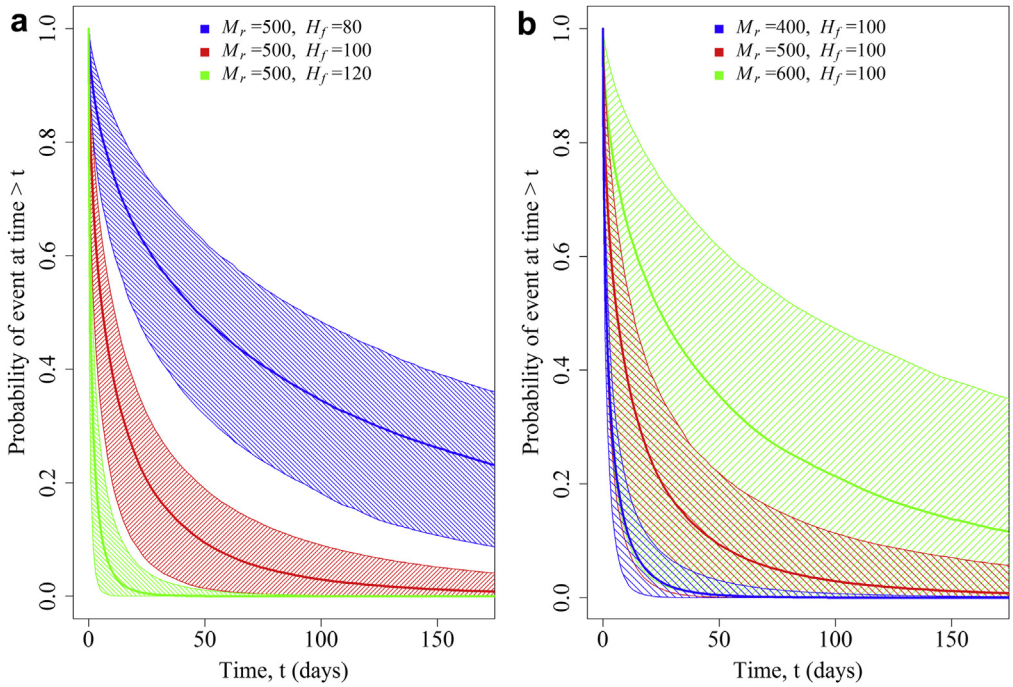

Figure 4. Sensitivity analysis showing differences in survival curves on changes in the model covariates. (a) M_r is constant and H_f changes by ±20%. (b) H_f is constant and M_r changes by ±20%. The colored areas show 80% confidence intervals based on percentiles.

for compounds outside the original 25 compound training set. Further details of the distributions of predicted crystallization event times are given in Supplementary Material E. We have previously correlated our experimentally observed amorphous stability values with those observed elsewhere using a range of different methodologies.[6] Furthermore, the relative amorphous stability ranges for the compounds in our validation data set (Table 5) are in line with the high (indoprofen[3,20,26]), intermediate (droperidol[3,26,33] and nifedipine[3,26,34]), and low (clotrimazole[3,26,34,35] and felodipine[3,26,34]) crystallization tendencies reported in the literature.

Although the representation of the model's predictive power given in Figure 5 indicates that the overall predictive performance is about as good as it could be expected, some of the individual predictions in Table 5 have large discrepancies. These discrepancies may be related to differences in preparation methods and storage conditions for the test set compounds compared with the compounds used in model building. For instance, felodipine was a member of the 25 compound training set[6] and classified as an unstable compound (measured crystallization within 5 days of storage) and was also a member of the test set where it had been assessed as a fairly stable compound (crystallization within 84 days).[3] It may be possible to further improve the model by including additional covariates in the future which have not yet been explored in the present study.

We should note that each of the 11 test set molecules represents a single sample from a corresponding large population of possible molecules, with each population having the appropriate pair of H_f and M_r values. Each of those populations will exhibit a range of amorphous stability. Furthermore, given the earlier discussion of the stochastic nature of TTE models, we can understand that the predicted crystallization times arise from distributions of values.

Table 4
Median Crystallization Times (days) for Different Combinations of H_f (J/g) and M_r (g/mol) Calculated Using Equation 10 and Parameter Estimates From Table 3

H_f \ M_r	300	350	400	450	500	550
50	63.2	128.8	262.3	534.1	1088	2215
60	22.5	45.8	93.3	190.1	387.1	788.3
70	8.01	16.31	33.21	67.6	137.7	280.5
80	2.85	5.80	11.82	24.07	49.02	99.83
90	1.01	2.07	4.21	8.57	17.4	35.53
100	0.36	0.74	1.50	3.05	6.21	12.64
110	0.13	0.26	0.53	1.09	2.21	4.50

Median crystallization times longer than 168 days are shaded in green (very stable compounds) and shorter than 1 week are shaded in red (very unstable compounds).

Table 5
Amorphous Stability Data for 11 Compounds Along With Prediction From MLR and TTE Models. Amorphous Stability Predicted With TTE Is Represented as the Median of the Simulated Event Times. Event Times Were Generated Up to 168 Days

Compound	Stability (d)		
	Observed	Predicted With MLR	Predicted With TTE
Indoprofen	0.004	1.63	0.02
Droperidol	1	5.13	0.7
Nifedipine	1	3.87	0.3
Clotrimazole	84	6.25	1
Felodipine	84	12.7	8
1	<14	12	16
2	5-14	8.3	11
3	<1	1	0.3
4	>40	1806.9	168
5	168	11.2	18
6	<1	123.6	168

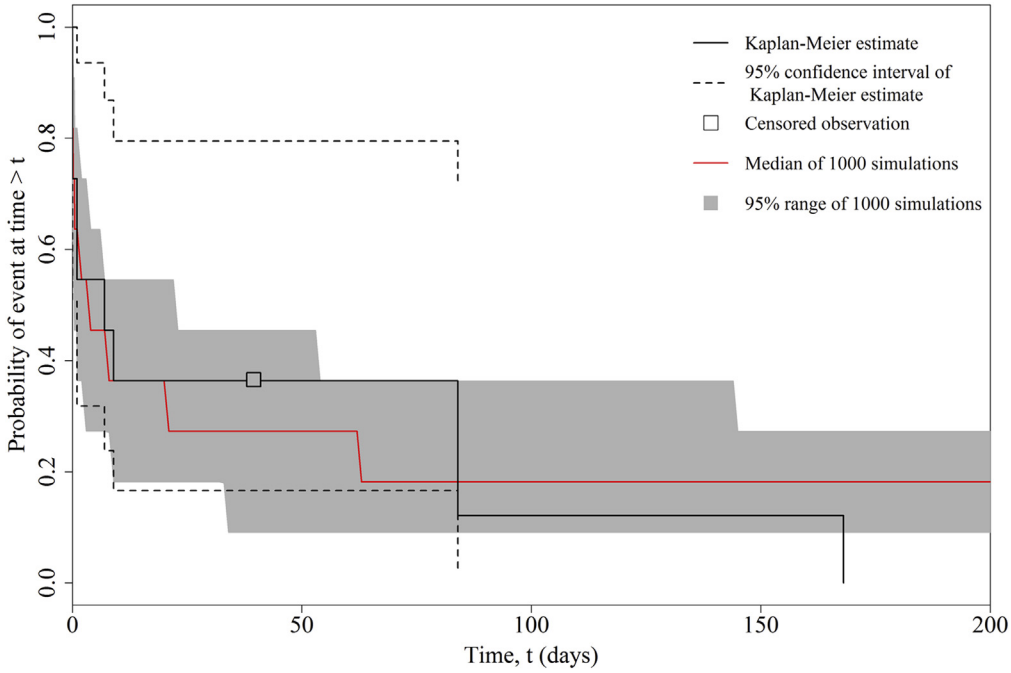

Figure 5. Assessment of predictive performance of the Weibull covariate model on 11 test set compounds.

Therefore, both, the observed and predicted crystallization times, should be viewed as having significant variability. The presence of some test set compounds with large discrepancy between the 2 times is to be expected. The variability in the predictions is tolerable as the derived model is not intended to replace the need for empirical drug stability studies and it would not be used in isolation to make critical decisions related to product development. The model should be rather viewed as a "risk assessment" tool to rank the relative amorphous stability of compounds, for example, in a discovery or early development setting, where there is a requirement from a biopharmaceutical or solid-state consideration for an amorphous drug formulation.

To compare the predictive abilities of the TTE model (Eq. 6) and the published MLR model (Eq. 7), the values of geometric mean-fold error (GMFE) and bias[36] were calculated for both models. These model predictivity metrics are listed in Table 6. The GMFE of the MLR model was 33% higher than the GMFE of the Weibull covariate model, and the bias was lower for the TTE model. This indicates that the predictive performance of the TTE model is better than the MLR model. This is consistent with the fact that a TTE analysis is, for several theoretical reasons, better suited to analysis of event versus time data (particularly given the interval-censored and right-censored nature of the data) than MLR.

Concluding Remarks

In this work, we discussed a novel application of TTE modeling to better understand the influence of physicochemical parameters on measured long-term amorphous stability with censored observations. This study used a previously published set of 25 representative poorly soluble compounds. The best description of the shape of the survival curve for the measured data was obtained with a Weibull hazard model consisting of 2 structural parameters, λ_1 and β_1. After investigating the effect of different physicochemical properties on λ_1 and β_1, the enthalpy of fusion (H_f) and molecular weight (M_r) significantly improved the model statistics. Using sensitivity analysis, it was shown that a decrease in H_f and an increase in M_r contribute to longer survival times of amorphous compounds and that amorphous stability depends more strongly on H_f than on M_r. The Weibull covariate model was used to calculate the median survival times for different values of H_f and M_r. The resulting survival times can serve as a useful indication of how amorphous drug stability typically responds to changes in H_f and M_r but with the realization that significant discrepancies are to be expected. Finally, the Weibull covariate model was tested on an external data set of 11 compounds and showed superior predictive power compared with a previously published MLR model, which also has a dependence on H_f and M_r. Because the 2 used covariates are readily accessible, through calculation and by means of differential scanning calorimetry, they may be of interest to the pharmaceutical industry in time- and cost-effective assessment of compound stability on storage and development of amorphous products. However, it will be beneficial to study additional compounds in the future to increase the data set and consequently reduce the uncertainty in the model parameter estimates.

Table 6
Metrics Comparing Predictive Performance of TTE and MLR Models When Tested on 11 External Compounds

Model	GMFE	Bias
MLR	10.10	1.63
TTE	6.73	−0.30

References

1. Newman A, Nagapudi K, Wenslow R. Amorphous solid dispersions: a robust platform to address bioavailability challenges. *Ther Deliv*. 2015;6(2):247-261.
2. Murdande SB, Pikal MJ, Shanker RM, Bogner RH. Solubility advantage of amorphous pharmaceuticals, part 3: is maximum solubility advantage experimentally attainable and sustainable? *J Pharm Sci*. 2011;100(10):4349-4356.
3. Baird JA, Van Eerdenbrugh B, Taylor LS. A classification system to assess the crystallization tendency of organic molecules from undercooled melts. *J Pharm Sci*. 2010;99(9):3787-3806.
4. Van Eerdenbrugh B, Raina S, Hsieh YL, Augustijns P, Taylor LS. Classification of the crystallization behavior of amorphous active pharmaceutical ingredients in aqueous environments. *Pharm Res*. 2014;31(4):969-982.

5. Graeser KA, Patterson JE, Zeitler JA, Gordon KC, Rades T. Correlating thermodynamic and kinetic parameters with amorphous stability. *Eur J Pharm Sci*. 2009;37(3-4):492-498.
6. Nurzyńska K, Booth J, Roberts CJ, McCabe J, Dryden I, Fischer PM. Long-term amorphous drug stability predictions using easily calculated, predicted and measured parameters. *Mol Pharm*. 2015;12:3389-3398.
7. Karmwar P, Graeser K, Gordon KC, Strachan CJ, Rades T. Investigation of properties and recrystallisation behaviour of amorphous indomethacin samples prepared by different methods. *Int J Pharm*. 2011;417(1-2):94-100.
8. Marsac PJ, Konno H, Taylor LS. A comparison of the physical stability of amorphous felodipine and nifedipine systems. *Pharm Res*. 2006;23(10):2306-2316.
9. Bhugra C, Pikal MJ. Role of thermodynamic, molecular, and kinetic factors in crystallization from the amorphous state. *J Pharm Sci*. 2008;97(4):1329-1349.
10. Mahlin D, Bergström CA. Early drug development predictions of glass-forming ability and physical stability of drugs. *Eur J Pharm Sci*. 2013;49(2):323-332.
11. Mahlin D, Ponnambalam S, Hockerfelt MH, Bergstrom CAS. Toward in silico prediction of glass-forming ability from molecular structure alone: a screening tool in early drug development. *Mol Pharm*. 2011;8(2):498-506.
12. Habgood M, Lancaster RW, Gateshki M, Kenwright AM. The amorphous form of salicylsalicylic acid: experimental characterization and computational predictability. *Cryst Growth Des*. 2013;13(4):1771-1779.
13. Ito A, Watanabe T, Yada S, et al. Prediction of recrystallization behavior of troglitazone/polyvinylpyrrolidone solid dispersion by solid-state NMR. *Int J Pharm*. 2010;383(1-2):18-23.
14. Hosmer DW, Lemeshow S, May S. *Applied Survival Analysis*. Hoboken, NJ: Wiley; 2008.
15. Holford N. A time to event tutorial for pharmacometricians. *CPT Pharmacometrics Syst Pharmacol*. 2013;2(5):1-8.
16. Owen JS, Fiedler-Kelly J. *Introduction to Population Pharmacokinetic/pharmacodynamic Analysis with Nonlinear Mixed Effects Models*. New York, NY: John Wiley & Sons; 2014.
17. Team RC. *R: A Language and Environment for Statistical Computing*. Vienna, Austria: R Foundation for Statistical Computing; 2014:2012. ISBN 3-900051-07-0.
18. Therneau T. *A Package for Survival Analysis in S. version 2.38*; 2013. Available at: http://CRAN.R-project.org/package=survival. Accessed April 10, 2016.
19. Soetaert K, Petzoldt T, Setzer RW. Solving differential equations in R. *RJ*. 2010;2:5-15.
20. Ueda H, Muranushi N, Sakuma S, et al. A strategy for co-former selection to design stable co-amorphous formations based on physicochemical properties of non-steroidal inflammatory drugs. *Pharm Res*. 2016;33(4):1018-1029.
21. Balakin KV, Savchuk NP, Tetko IV. In silico approaches to prediction of aqueous and DMSO solubility of drug-like compounds: trends, problems and solutions. *Curr Med Chem*. 2006;13(2):223-241.
22. Veber DF, Johnson SR, Cheng H-Y, Smith BR, Ward KW, Kopple KD. Molecular properties that influence the oral bioavailability of drug candidates. *J Med Chem*. 2002;45(12):2615-2623.
23. Taylor LS, Zografi G. Spectroscopic characterization of interactions between PVP and indomethacin in amorphous molecular dispersions. *Pharm Res*. 1997;14(12):1691-1698.
24. Bender R, Augustin T, Blettner M. Generating survival times to simulate Cox proportional hazards models. *Stat Med*. 2005;24(11):1713-1723.
25. Mould D, Upton R. Basic concepts in population modeling, simulation, and model-based drug development—Part 2: introduction to pharmacokinetic modeling methods. *CPT Pharmacometrics Syst Pharmacol*. 2013;2(4):1-14.
26. Baird JA, Thomas LC, Aubuchon SR, Taylor LS. Evaluating the non-isothermal crystallization behavior of organic molecules from the undercooled melt state using rapid heat/cool calorimetry. *Cryst Eng Comm*. 2013;15(1):111-119.
27. Byon W, Smith M, Chan P, et al. Establishing best practices and guidance in population modeling: an experience with an internal population pharmacokinetic analysis guidance. *CPT Pharmacometrics Syst Pharmacol*. 2013;2(7):1-8.
28. Mandema JW, Verotta D, Sheiner LB. Building population pharmacokinetic-pharmacodynamic models. I. Models for covariate effects. *J Pharmacokinet Biopharm*. 1992;20(5):511-528.
29. Lindbom L, Ribbing J, Jonsson EN. Perl-speaks-NONMEM (PsN)—a Perl module for NONMEM related programming. *Comput Methods Programs Biomed*. 2004;75(2):85-94.
30. Vu TC, Nutt JG, Holford NH. Disease progress and response to treatment as predictors of survival, disability, cognitive impairment and depression in Parkinson's disease. *Br J Clin Pharmacol*. 2012;74(2):284-295.
31. Karlsson M, Savic R. Diagnosing model diagnostics. *Clin Pharmacol Ther*. 2007;82(1):17-20.
32. Holford N. The visual predictive check—Superiority to standard diagnostic (Rorschach) plots. Conference abstract 738. Pamplona, Spain; 2005; 14. Available at: http://www.page-meeting.org/?abstract=738. Accessed April 21, 2016.
33. Trasi NS, Baird JA, Kestur US, Taylor LS. Factors influencing crystal growth rates from undercooled liquids of pharmaceutical compounds. *J Phys Chem B*. 2014;118(33):9974-9982.
34. Alhalaweh A, Alzghoul A, Mahlin D, Bergström CA. Physical stability of drugs after storage above and below the glass transition temperature: relationship to glass-forming ability. *Int J Pharm*. 2015;495(1):312-317.
35. Pajula K, Taskinen M, Lehto V-P, Ketolainen J, Korhonen O. Predicting the formation and stability of amorphous small molecule binary mixtures from computationally determined Flory–Huggins interaction parameter and phase diagram. *Mol Pharm*. 2010;7(3):795-804.
36. Lombardo F, Waters NJ, Argikar UA, et al. Comprehensive assessment of human pharmacokinetic prediction based on in vivo animal pharmacokinetic data, part 2: clearance. *J Clin Pharm*. 2013;53(2):178-191.